Journal of Applied Electrochemistry **33**: 367–372, 2003.

Anodic linear sweep voltammetric analysis of Ni–Co alloys electrodeposited from dilute sulfate baths

A.N. CORREIA[1] and S.A.S. MACHADO[2,*]
[1]*Departamento de Química Analítica e Físico-Química, Universidade Federal do Ceará, Bloco 940, Campus do Pici, 60451-970, Fortaleza, CE, Brazil*
[2]*Departamento de Físico-Química, Instituto de Química de São Carlos, Universidade de São Paulo, Cx.P. 780, 13560-970, São Carlos, SP, Brazil*
*(*author for correspondence, fax: +55 16 273 9952, e-mail: sasmach@iqsc.sc.usp.br)*

Received 8 January 2002; accepted in revised form 10 January 2003

Key words: electrodeposition, linear sweep voltammetry, morphological aspects, Ni–Co alloys, sulfate baths

Abstract

Anodic linear sweep voltammetry was used to characterise electrodeposits of Ni, Co and five Ni–Co alloys (5:1, 2:1, 1:1, 1:2 and 1:5 ratios) obtained in a potentiodynamic mode on a vitreous carbon electrode from dilute sulfate baths. The voltammetric results showed a complex behaviour, with the deposits strongly dependent on the metal ion concentrations and less dependent on the final deposition potential. Probably due to simultaneous hydrogen evolution, the efficiency of the electrodeposition (in sulfate baths) and electrodissolution (in ammoniacal bath) processes of pure Co and Ni–Co alloys decreased with increasing final potential in all solutions, while that of pure Ni was enhanced with a shift to more negative potentials. Morphological information was acquired through investigations by techniques such as SEM, EDX and dot mapping. The voltammetric results revealed solid solution characteristics, with profiles varying from pure Ni to pure Co. The results of semi-quantitative EDX chemical analyses suggest a regular deposition mechanism instead of an anomalous one as is often observed in such binary systems.

1. Introduction

Electrodeposition techniques are widely used to produce metallic alloy layers [1–10], mainly because they represent a less costly alternative to other deposition methods such as physical and chemical vapor deposition (PVC and CVD). For protective coatings, electrodeposition methodologies present additional advantages involving enhanced control of the alloy composition, as well as coating thickness and shape. Moreover, unlike vapor phase-produced coatings, which are often porous, electrodeposits can be made more compact, which enhances their corrosion resistance [11].

Unlike those obtained by metallurgical processes [12], thin layers of electrodeposited alloys possess several characteristic properties. These layers are known to commonly consist of different phases, including compounds of the main metallic components (e.g., oxides) and impurities formed of the alloying elements [13].

Anodic linear sweep voltammetry (ALSV) is a well-established technique to identify the different phases commonly present in most alloy systems [14–27]. ALSV characteristics, in particular, are highly sensitive to the characteristics of electrodeposits. It has been demonstrated that anodic dissolution can be considered a 'fingerprint' of thin alloy layers [23]. This method appears to be a suitable alternative since the appropriate technique to analyse crystal structures (i.e., X-ray analysis), is restricted insofar as the identification of thin films on amorphous substrates, such as vitreous carbon, is concerned.

Although the literature contains extensive studies of different types of alloy, few papers report on Ni–Co [28–35]. An earlier paper from our laboratory [36] reported on a study of the electrodeposition of Ni–Co alloys on a glassy carbon substrate from dilute chloride baths. That study revealed voltammetric results displaying a complex behaviour, with the deposit strongly dependent on the metal ion concentrations in the bath and on the final deposition potential. The experimental results for five alloy ratios showed electrochemical and physical behaviours varying from the kind associated with pure Ni to that associated with pure Co. Quantitative chemical analyses confirmed that, under our experimental conditions, a regular rather than an anomalous deposition mechanism occurred.

However, some authors suggest the possible influence of anionic species in electrodeposition/electrodissolution

processes [37–40]. In the present study, dilute sulfate baths were used to obtain Ni–Co electrodeposits under controlled conditions, followed by stripping experiments to characterise the thin Ni–Co films. The electrochemical and physical results were also interpreted as a function of the deposition potential and bath composition. Thus, in view of the complexities associated with electrodeposited alloys, the results were correlated with those previously reported in a chloride medium [36].

2. Experimental procedure

The chemical products (Merck PA reagents) used in this study were 0.01 mol dm^{-3} $NiSO_4$ + 0.1 mol dm^{-3} Na_2SO_4 or 0.01 mol dm^{-3} $CoSO_4$ + 0.1 mol dm^{-3} Na_2SO_4 electrolytes, while the alloys were obtained from baths containing Ni(II)/Co(II) ratios of 5:1 (i.e., 0.05 mol dm^{-3} $NiSO_4$ + 0.01 mol dm^{-3} $CoSO_4$ + 0.1 mol dm^{-3} Na_2SO_4), 2:1, 1:1, 1:2 and 1:5, all in pH 6.4. The stripping analyses were performed in 0.5 mol dm^{-3} NH_4Cl. All the solutions were freshly prepared with water treated in a Millipore Milli-Q system. In these experiments, the electrolyte solution was bubbled with purified nitrogen (White Martins SS) for at least 15 min prior to the experiments and the atmosphere was kept constant during the experiments in order to remove O_2. All the experiments were performed at room temperature.

Electrochemical experiments were carried out in a conventional three-electrode cell using an EG&G PARC model 273 potentiostat/galvanostat controlled by a PC type microcomputer with a GPIB card containing M270 software. The working electrode (0.2 cm^2 geometric area) was a vitreous carbon rod (CTA, Brazil). This electrode was hand-polished to a mirror finish before each experiment using emery papers (up to grid 2000). The auxiliary electrode was a Pt sheet with a 2 cm^2 geometric area and the reference system was a saturated calomel electrode (SCE).

The surface morphology of the electrodeposit was examined with a DSM 960 (Carl Zeiss) scanning electron microscope. The qualitative and semiquantitative chemical analyses of the alloys were performed by energy dispersive X-ray (EDX) in a model QX 2000 (Link Analytical) device using Ni and Co standards (99.998%) from Micro-Analysis Consultants Ltd (Cambridgeshire, UK).

Metal electrodepositions were carried out by potential scanning from 1.0 V to a final potential varying between −0.9 and −1.3 V, at 5 mV s^{-1}, in the corresponding electrolyte.

The stripping analysis was consistently made immediately after deposition, also at 5 mV s^{-1}, but in the stripping solution given above. In this case, the initial potential always coincided with the final potential of the electrodeposition curve and the positive scan was stopped at 1.0 V. Only one deposition or dissolution cycle was run for each experiment.

3. Results and discussion

To gain a better understanding of the electrodeposition and electrodissolution processes of Ni–Co alloys, a preliminary study was made of the deposition of pure metals in a simple sulfate bath. The voltammetric responses were also used to interpret the more complex Ni–Co profiles.

3.1. *Cyclic voltammetry*

Cyclic voltammograms for Ni (dashed line), Co (dotted line) and Ni–Co 1:1 (full line) deposition/dissolution in 0.01 mol dm^{-3} $NiSO_4$ + 0.1 mol dm^{-3} Na_2SO_4, 0.01 mol dm^{-3} $CoSO_4$ + 0.1 mol dm^{-3} Na_2SO_4 and 0.005 mol dm^{-3} $NiSO_4$ + 0.005 mol dm^{-3} $CoSO_4$ + 0.1 mol dm^{-3} Na_2SO_4 electrolytes, respectively, are shown in Figure 1. The current scale was divided by an *f* factor, taking into account the increased metal ion concentration in the electrolyte used for the alloy deposition experiments. Thus, the *f* factor was set at 2 for Ni–Co 1:1 and at 1 for the individual metals. Two crossovers of current were detected in the negative scan, which are commonly associated with electrocrystallization processes involving increases in surface area. In each voltammetric profile, the respective reduction process presented a single peak whose onset shared the same potential value. After reaching a peak, the currents decreased according to a diffusion-controlled process. On the other hand, the cathodic peaks appeared at somewhat different potentials, that is, −0.95 V, −0.85 V and −0.90 V for Ni, Co and Ni–Co, respectively. Moreover, the peak current for the Co deposition was larger than those for Ni or Ni–Co, which was probably due to the fact that the deposition rate for Co was faster than for the other systems. Contrary to what was observed in chloride medium [36], the alloy deposition in sulfate electrolyte showed an intermediate behaviour in relation to the peak potential and current values. On positive scans, only Co deposits presented the corre-

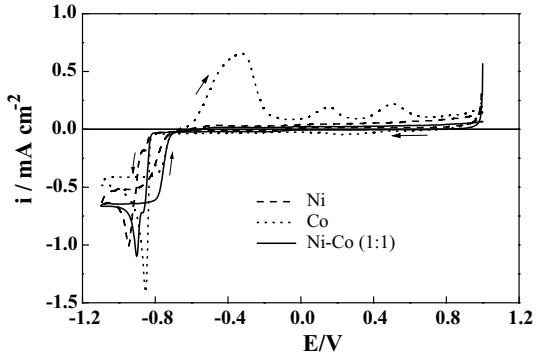

Fig. 1. First-cycle voltammograms for vitreous carbon electrode in 0.01 mol dm^{-3} $NiSO_4$ + 0.1 mol dm^{-3} Na_2SO_4 (- - - -), 0.01 mol dm^{-3} $CoSO_4$ + 0.1 mol dm^{-3} Na_2SO_4 (· · · · ·) and 0.005 mol dm^{-3} $NiSO_4$ + 0.005 mol dm^{-3} $CoSO_4$ + 0.1 mol dm^{-3} Na_2SO_4 (——) solutions at 5 mV s^{-1}.

sponding dissolution process with three current maxima, while Ni and Ni–Co alloys showed no evidence of a dissolution process, in this potential region, maybe due to the enhanced stability of Ni surfaces in non-acid media.

3.2. *Electrodeposition experiments*

With the aim of producing different Ni–Co alloy compositions on the electrode surface, electrodepositions were made by potential scanning from 1.0 V to different final potential values of −0.9 V, −1.0 V, −1.1 V, −1.2 V and −1.3 V, at 5 mV s^{-1}, in the several different electrolytic solutions described earlier. Scanning the potential up to −1.1 V in all the electrolytes generated voltammetric profiles similar to those previously found in chloride medium [36]. The deposition processes presented a single maximum whose peak potential values varied arbitrarily between −0.88 (Ni–Co 1:2) and −0.95 V (Ni–Co 5:1). Such behaviour may be associated with variations in the experimental conditions such as the total ionic concentration, ionic strength of the solution, local pH, etc. Finally, excursions for potential values more negative than −1.1 V gave extensive hydrogen evolution, which was demonstrated by the exponential growth of the current values [9, 39–41]. The electrodeposits produced with this procedure were further examined by electrochemical and physical techniques in order to analyse their compositions.

3.3. *ALSV results*

It has been shown that the ALSV technique is a suitable electrochemical tool [14–27] for the characterization of electrochemically obtained thin layers of metallic alloys. Under anodic polarisation conditions, the distinct components of an alloy tend to dissolve at different potentials, and the distribution of voltammetric peaks is characteristic for each alloy structure. The peak currents depend on the film thickness, while their number and potentials depend only on the alloy structure.

The experimental procedure used was similar to that described in [36]. Here, the dissolution experiments were carried out in 0.5 mol dm^{-3} NH_4Cl at 5 mV s^{-1}. Figure 2 illustrates the ALSV responses for dissolution of pure Ni and Co electrodeposited during potential scanning up to −0.9 V (solid line), −1.1 V (dash dot line) and −1.3 V (dotted line). In contrast to the behaviour observed in sodium sulfate medium, both Ni and Co dissolve in the highly complex ammonium electrolyte. Figure 2 shows two dissolution peaks for Ni stripping and one for Co. The peak potential for the highest peak showed similar values in both cases, that is, 0.38 V for Ni and 0.42 V for Co. Because of the faster deposition kinetics of Co, higher dissolution charges were detected than for Ni at identical final potential values. However, for depositions up to −0.9 V, Ni

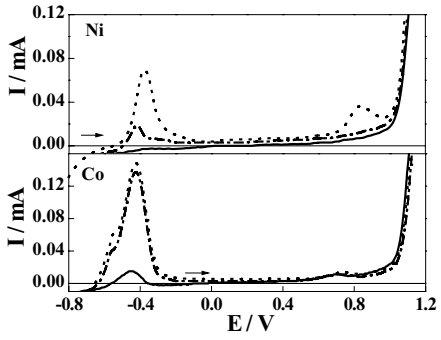

Fig. 2. Anodic linear sweep voltammograms in 0.5 mol dm^{-3} NH_4Cl at 5 mV s^{-1} for Ni and Co electrodeposits obtained from the sulfate baths gives in Figure 1 by potential sweep up to −0.9 V (solid line), −1.1 V (dash-dot line) and −1.3 V (dotted line).

deposits failed to show any dissolution current. On the other hand, with a scan of up to −1.3 V, the Ni deposit formed under intense hydrogen evolution showed a new dissolution peak at approximately 0.85 V, which can be associated to the formation of Ni phases with different characteristics under such reducing conditions (which can even induce hydrogen incorporation in Ni deposits). Moreover, the Co dissolution charges seem to stabilize around −1.1 V, probably due to hydrogen evolution at more negative potentials.

Although it is well known that nickel and cobalt form solid solutions at the atomic level over the entire composition range [1, 42], a clear difference was found in the corresponding stripping voltammograms for the alloys and the pure metals, as shown in Figure 3, in which the current scale was again corrected by the f factor. For 5:1 Ni–Co alloy, a unique oxidation peak was observed at −0.25 V, presenting characteristics similar to those observed for Ni deposits, that is, an absence of oxidation currents for deposits obtained up to −0.9 V and a peak potential close to that of Ni. However, there is evidence that these deposits differ from pure Ni, that is, the absence of the peak at 0.8 V and the higher values of dissolution charge than that shown in Figure 2.

This dissolution behaviour altered dramatically in the Ni–Co 2:1 alloy, in which three peaks appeared in the anodic scan, the first one around −0.4 V, the second near 0.4 V and the last at approximately 0.6 V, as shown in Figure 3. The dissolution charges were much smaller than that observed in the 5:1 alloy. This change in voltammetric profile may be associated with the somewhat different alloy compositions obtained for the 5:1 and 2:1 Ni–Co electrodeposits.

The changes in voltammetric profiles were reduced by increasing the alloy Co content. For 1:1 and 1:2 Ni–Co alloys, the first peak at −0.4 V tended to diminish while those around 0.4 V increased and shifted toward less positive potentials.

Three dissolution peaks were again observed in the 1:5 Ni–Co alloy response. Here, the peak around −0.4 V reappeared, as did the one at 0.0 V, both of which were

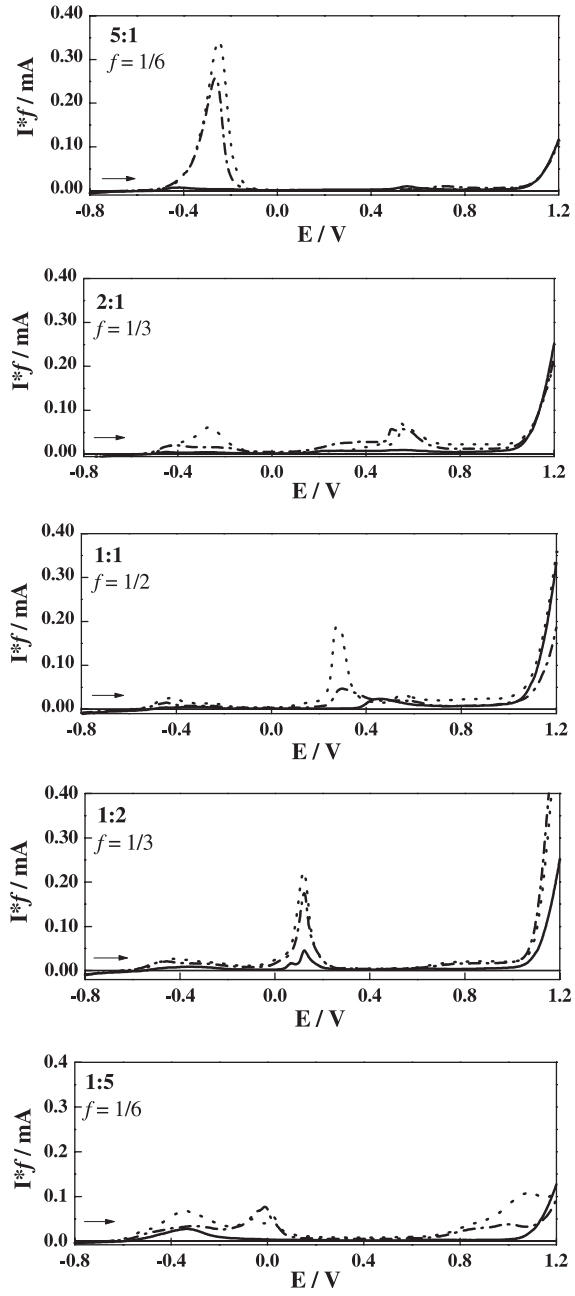

Fig. 3. Anodic linear sweep voltammograms in 0.5 mol dm^{-3} NH_4Cl at 5 mV s^{-1} for electrodeposits of Ni–Co alloys (as indicated) obtained from the five different sulfate baths (see text) by negative sweep up to −0.9 V (solid line), −1.1 V (dash-dot line) and −1.3 V (dotted line).

attributed to an excess of Co when related to the Ni content of the alloy, while a new peak around 1.0 V was associated with the reduced Ni dissolution shown in Figure 2.

All these variations, which appear to be only slightly dependent on the final potential of the deposition scan in the range −0.9 to −1.3 V, indicate that the assumption of the formation of a simple solid solution does not, *per se*, justify the response of Ni–Co alloys, since it should give rise to only one dissolution peak, whose potential should vary smoothly with parameters such as pH, ionic strength and electrolyte composition. Hence, based in the number and behaviour of the voltammetric peaks observed, it must be assumed that there are several intermetallic compositions.

The current efficiency (η) for each alloy was determined as the ratio between the charge obtained under the ALSV peaks (in the ammoniacal bath) (Q_{anod}) and the charge passed during the deposition experiments (in sulfate baths) (Q_{cat}). Table 1 lists the dependences of η on the final potential of the deposition scan (−0.9 to −1.3 V). It can be observed that, for Co electrodeposition, the hydrogen evolution exerts an increasing influence with potential incursion towards negative values, lowering the current efficiencies. On the other hand, Ni electrodeposition behaves in an opposite way. The current efficiency increases when the potential becomes negative. This is probably associated with deposition, at more negative potentials, of less organized films, which are more susceptible to oxidation yielding higher oxidation currents in the ALSV experiments. The dissolution currents for pure Ni deposits are up to −1.1 V, smaller than those for pure Co films, as can be seen in Figure 2. The potential scanning for −1.3 V generates Ni films with dissolution currents closer to those for Co at the same final potential.

3.4. *Physical characterization*

The morphological aspects of Ni, Co and Ni–Co alloys deposited on vitreous carbon electrodes from sulfate baths at a potential sweep of up to −1.1 V were examined by SEM. Figure 4 shows that different microstructures and, hence, alloy compositions were obtained for the different bath composition.

Figure 4 shows that Ni electrodeposits have a highly irregular platelet structure, while Co presents a more ordered fibrilar one. The same structures had been observed in Ni and Co electrodeposits obtained from a chloride bath [36]. By increasing the amount of cobalt in

Table 1. Values of current efficiency for the electrodeposition processes of pure Ni, Ni–Co alloys and pure Co

$-E_{inv}$ /V	Q_{anode}/Q_{cat}						
	Ni	5:1	2:1	1:1	1:2	1:5	Co
0.9	0.16	0.79	0.71	0.73	0.79	0.85	0.43
1.0	0.27	0.87	0.74	0.45	0.69	0.75	0.66
1.1	0.29	0.83	0.69	0.48	0.67	0.73	0.65
1.2	0.30	0.70	0.61	0.61	0.62	0.64	0.56
1.3	0.34	0.59	0.45	0.48	0.52	0.58	0.43

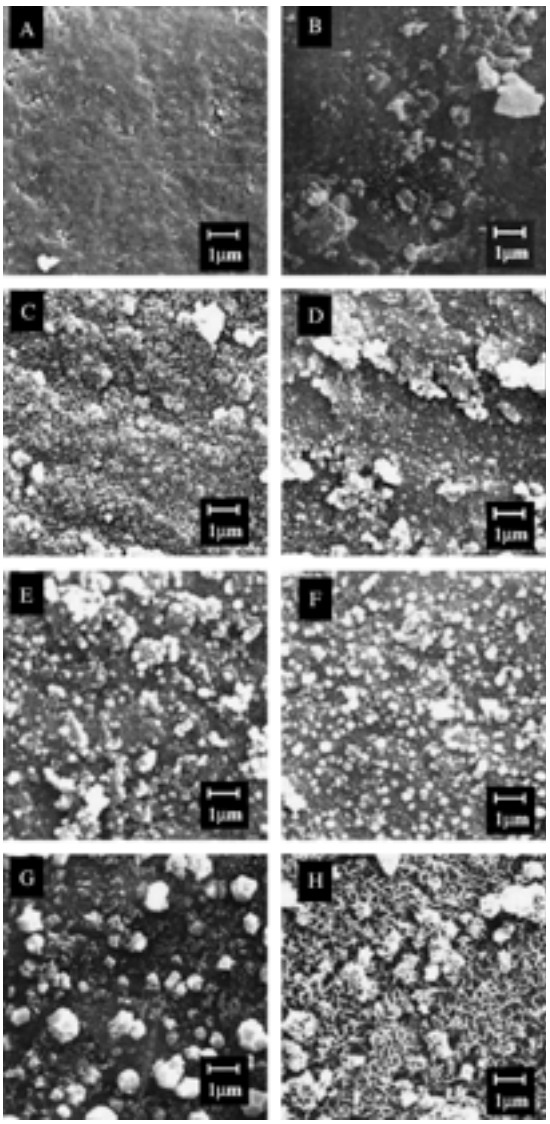

Fig. 4. SEM micrographs for electrodeposits obtained by linear sweep voltammetry up to −1.1 V for the different Ni–Co alloys: (A) Substrate, (B) Ni, (C) 5:1, (D) 2:1, (E) 1:1, (F) 1:2, (G) 1:5 and (H) Co.

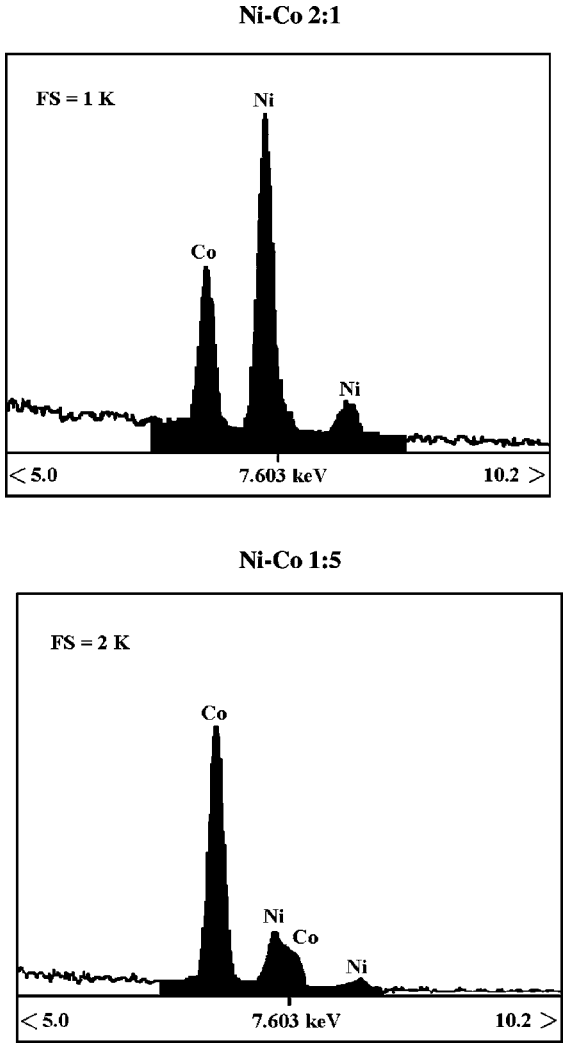

Fig. 5. EDX spectra for two compositions of Ni–Co alloys electrodeposited by linear sweep voltammetry up to −1.1 V. Ni–Co compositions: 2:1 (upper) and 1:5 (lower).

Table 2. Comparison between theoretical and experimental values for the pure Ni, Ni–Co alloys and pure Co in the electrolytic solutions with the metallic percentage in the electrodeposits found by EDX. Linear sweep up to −1.1 V

System	Theoretical		Experimental	
	% Ni	% Co	% Ni	% Co
Pure Ni	100.0	0	100.0	0
Ni–Co 5:1	83.3	16.7	80.0	20.0
Ni–Co 2:1	66.7	33.3	69.0	31.0
Ni–Co 1:1	50.0	50.0	54.0	46.0
Ni–Co 1:2	33.3	66.7	37.0	63.0
Ni–Co 1:5	16.7	83.3	20.0	80.0
Pure Co	0	100.0	0	100.0

the electrolyte, the morphologies of the deposited thin layer of Ni–Co alloys underwent a progressive change, varying from a fibrilar Co-like structure, in the case of the 1:5 alloy, to globular platelet-like deposits in 1:2, 1:1, 2:1 and 5:1 alloys. From these SEM images, it can be concluded that the morphological appearance of Ni–Co alloys changes, when the Co content of the bath is increased, passing from that of pure Ni to the microstructure obtained for pure Co.

Because the Ni, Co and Ni–Co alloys deposited during the potential scan up to the same final potential on vitreous carbon electrode showed morphological differences, the electrodeposits were subjected to a semiquantitative X-ray dispersion analysis to verify the correlation between the bath composition and the amount of codeposited nickel and cobalt. Figure 5 presents EDX spectra for both 2:1 and 1:5 alloys obtained for a −1.1 V final potential. A comparison of the height of the Ni–Co signals and the metal ion concentration in the electrolytic solutions reveals that Ni–Co codeposition follows a regular mechanism, and not an anomalous one, under all the experimental conditions used. The results for all the Ni–Co alloys are compiled in Table 2, which shows the same nickel and cobalt percentages in the electrolytic bath and in the deposits. This finding disagrees with some authors [28, 30, 31, 33], who postulated an

anomalous Ni–Co deposition mechanism under several experimental conditions.

Finally, EDX dot-mapping experiments were performed to visualize the distribution of alloy components in the Ni–Co layer. It was noted that the deposition is highly homogeneous, with no preferential surface region for nickel or cobalt deposition for all Ni–Co compositions.

4. Conclusions

Electrochemical dissolution experiments on Ni–Co alloys and SEM analyses revealed a strong dependence of alloy compositions on the concentration of metallic ions in the deposition bath. The electrodeposits obtained from bath with different percentage of Ni^{2+} and Co^{2+} ions yielded varying number of peaks in different potentials in the ALSV experiments in NH_4Cl medium. Since in such experiments multiple peaks are usually associated to the dissolution of distinct alloy phases, these variations evidenced the formation of several Ni–Co species, which is also supported by the SEM analysis which shows different Ni and Co content in each deposit. The nature of such alloys was found to be only slightly dependent on the final potential during deposition scanning. On the other hand, an almost homogeneous change in voltammetric and morphologic aspects was observed to occur from low to high Co content alloy, produced by increasing amounts of Co(II) in the electrolyte. These observations points to the formation of different intermetallic alloys with intermediate compositions of Ni and Co. Finally, the chemical analysis with EDX showed a regular deposition mechanism, with the alloy composition directly dependent on bath composition. This is contrary to some published results, which suggest that Ni–Co codeposition has an anomalous mechanism, in which Co (the less noble component) deposits preferentially.

Acknowledgements

The authors are indebted to the Conselho Nacional de Desenvolvimento Científico e Tecnológico (CNPq), Brazil.

References

1. K.M. Gorbunova and Yu.M. Polukarov, *in* C.W. Tobias (Ed.), 'Advances in Electrochemistry and Electrochemical Engineering', Vol. 5 (J. Wiley & Sons, New York, 1976), p. 249.
2. E. Chassaing and R. Wiart, *Electrochim. Acta* **37** (1992) 545.
3. A.S.M.A. Haseeb, J.P. Celis and J.R. Roos, *J. Electrochem. Soc.* **141** (1994) 230.
4. A. Stankeviciute, K. Leinartas, G. Bikulcius, D. Virbalyte, A. Sudavicius and E. Juzeliunas, *J. Appl. Electrochem.* **28** (1998) 89.
5. F. Elkhatabi, M. Benballa, M. Sarret and C. Müller, *Electrochim. Acta* **44** (1999) 1645.
6. I. Petersson and E. Ahlberg, *J. Electroanal. Chem.* **485** (2000) 166.
7. I. Petersson and E. Ahlberg, *J. Electroanal. Chem.* **485** (2000) 178.
8. S. Armyanov, *Electrochim. Acta* **45** (2000) 3323.
9. C. Müller, M. Sarret and M. Benballa, *Electrochim. Acta* **46** (2001) 2811.
10. P. Chen and I. Sun, *Electrochim. Acta* **46** (2201) 1169.
11. K.E. Heusler, *Corros. Sci.* **39** (1997) 1177.
12. A. Brenner, 'Electrodeposition of Alloys, Principles and Practice', Vols. 1 and 2 (Academic Press, New York, 1963).
13. Ya.M. Kolotyrkin, *Electrochim. Acta* **25** (1980) 89.
14. S. Swathirajan, *J. Electrochem. Soc.* **133** (1986) 671.
15. S. Swathirajan, *J. Electroanal. Chem.* **221** (1987) 221.
16. V.D. Jovic, R.M. Zejnilovic, A.R. Despic and J. Stevanovic, *J. Appl. Electrochem.* **18** (1988) 511.
17. V.D. Jovic, A.R. Despic, J.S. Stevanovic and S. Spaic, *Electrochim. Acta* **34** (1989) 1093.
18. V.D. Jovic, B.M. Jovic and A.R. Despic, *J. Electroanal. Chem.* **357** (1992) 357.
19. C.Q. Cui and A.C.C. Tseung, *J. Electrochem. Soc.* **139** (1992) 3390.
20. J.S. Stevanovic, V.D. Jovic and A.R. Despic, *J. Electroanal. Chem.* **349** (1993) 365.
21. F. Elkhatabi, M. Sarret and C. Muller, *J. Electroanal. Chem.* **404** (1996) 45.
22. F. Elkhatabi, G. Barceló, M. Sarret and C. Muller, *J. Electroanal. Chem.* **419** (1996) 71.
23. J.S. Stevanovic, A.R. Despic and V.D. Jovic, *Electrochim. Acta* **42** (1997) 873.
24. S.K. Zecevic, J.B. Zotovic, S.Lj. Gojkovic and V. Radmilovic, *J. Electroanal. Chem.* **448** (1998) 245.
25. E. Gómez, X. Alcobe and E. Vallés, *J. Electroanal. Chem.* **475** (1999) 66.
26. E. Gómez, A. Llorente and E. Vallés, *J. Electroanal. Chem.* **495** (2000) 19.
27. E. Gómez, X. Alcobe and E. Vallés, *J. Electroanal. Chem.* **505** (2001) 54.
28. S.S. Abd El-Rehim, A.M. Abd El-Halim and M.M. Osman, *J. Appl. Electrochem.* **15** (1985) 107.
29. I. Arul Raj and K.I. Vasu, *J. Appl. Electrochem.* **20** (1990) 32.
30. P.C. Andricacos, *J. Electrochem. Soc.* **142** (1995) 1824.
31. C. Fan and D.L. Piron, *Electrochim. Acta* **41** (1996) 1713.
32. B. Lochel and A. Maciossek, *J. Electrochem. Soc.* **143** (1996) 3343.
33. V.D. Jovic, N. Tosic and M. Stojanovic, *J. Electroanal. Chem.* **420** (1997) 43.
34. D. Golodnitsky, N.V. Gudin and G.A. Volyanuk, *Plat. Surf. Finish.* **85** (1998) 65.
35. S. Goldbach, R. de Kermadec and F. Lapicque, *J. Appl. Electrochem.* **30** (2000) 277.
36. A.N. Correia and S.A.S. Machado, *Electrochim. Acta* **45** (2000) 1733.
37. J.R. Roos, J.P. Celis and M. de Bonte, *in* R.W. Cahn, P. Haasen and E.J. Kramer (Eds), 'Materials Science and Technology, A Comprehensive Treatment', Vol. 15 (Wiley–VCH, Weinheim, 1991), p. 480.
38. D. Landolt, *Electrochim. Acta* **39** (1994) 1075.
39. R. Winand, *Electrochim. Acta* **39** (1994) 1091.
40. M. Ishikawa, H. Enomoto, M. Matsuoka and C. Iwakura, *Electrochim. Acta* **40** (1995) 1663.
41. A.B. Soto, E.M. Arce, M. Palomar-Pardavé and I. González, *Electrochim. Acta* **41** (1996) 2647.
42. A.R. Despic and V.D. Jovic, *in* R.E. White, J.O'M. Bockris and B.E. Conway (Eds), 'Modern Aspects of Electrochemistry', Vol. 27 (Plenum Press, New York, 1995), p. 143.